Proposal for on-chip generation and control of photon hyperentanglement

S. V. Zhukovsky,[1,2,*] D. Kang,[2] P. Abolghasem,[2] L. G. Helt,[1] J. E. Sipe,[1] and A. S. Helmy[2]

[1]*Department of Physics and Institute for Optical Sciences, University of Toronto, 60 St. George Street, Toronto, Ontario M5S 1A7, Canada*

[2]*The Edward S. Rogers Department of Electrical and Computer Engineering, University of Toronto, 10 Kings College Road, Toronto, Ontario M5S 3G4, Canada*

**Corresponding author: szhukov@physics.utoronto.ca*

Received June 24, 2011; revised August 11, 2011; accepted August 11, 2011; posted August 16, 2011 (Doc. ID 149827); published September 8, 2011

An on-chip waveguide-based source of entangled photons capable of switching between generating time-energy entangled and hyperentangled (entangled in both time energy and polarization) photon pairs is proposed. The switching can be done all-optically by rotating the pump polarization. The source is based on multichannel phase matching in Bragg reflection waveguides achieved by engineering the Fresnel reflection of photonic bandgap claddings for differently polarized modes. Analytical results are confirmed in fully vectorial numerical simulations.

OCIS codes: 230.7380, 230.1480, 050.2555.

Entanglement is the enabling phenomenon behind many aspects of quantum communication and information processing, such as cryptography, dense coding, teleportation, and quantum logic element design [1–3]. It is also a crucial phenomenon for testing the fundamentals of quantum theory, e.g., the violation of Bell's inequalities. Entangled photons are particularly suitable for communication applications because of their long coherence times and a high propagation speed as well as because of their easy generation by spontaneous parametric downconversion (SPDC) in $\chi^{(2)}$-nonlinear crystals [2].

The mainstream approach to investigating and utilizing entanglement has been to focus on one degree of freedom (DOF), eliminating the dependence of the quantum state on other DOFs. Being the most accessible and controllable, polarization-entangled photon pairs are the most studied [4], but other discrete (e.g., mode number) and continuous DOFs (e.g., frequency or transverse momentum) can also be used [3,5]. In fact, generated photons are often entangled in more than one DOF, or *hyperentangled* [6]. Such states can improve the reliability of quantum interference experiments [7] and have other uses in quantum information [8–10].

Being able to integrate entangled photon sources with other components on an optical chip is pivotal in making quantum communication devices more practical. A number of on-chip entangled photon sources suitable for such integration have been reported [11–13], as well as approaches for on-chip interferometry [2,5,14] and quantum logic gate design [15]. As there may be fewer DOFs in a channel waveguide than in free space, it is desirable to have flexibility with respect to which DOFs are used to separate the photons and which carry the entanglement. One also needs to be able to characterize and control hyperentanglement [16] on a chip.

The two most common SPDC scenarios involve type I and type II phase matching (PM), producing copolarized and cross-polarized entangled photons, respectively. In a channel where both photons are copropagating and do not have the DOF of transverse momentum, type I PM with a cw pump produces photons having just the time-energy entanglement, with the state roughly described by $|\omega_h\omega_l\rangle + |\omega_l\omega_h\rangle$, where ω_l and ω_h denote low- and high-frequency photons. Type II PM produces states with both time-energy and polarization entanglement, i.e., $(|\mathrm{HV}\rangle + |\mathrm{VH}\rangle) \otimes (|\omega_h\omega_l\rangle + |\omega_l\omega_h\rangle)$, which are in this sense hyperentangled.

These two PM types can coexist in the same structure [17], involving different polarization of the pump light. Hence, the two kinds of photon states (hyperentangled and time-energy entangled) can be switched by rotating the pump polarization without any external tuning mechanism if we make the two PM types manifest at the same pump wavelength. In this Letter, we theoretically demonstrate such switching in a channel-waveguide structure designed to have two types of PM (type I + type II or type 0 + type II). By continually changing the pump polarization, the degree of polarization entanglement in the hyperentangled state can be gradually varied, which is a convenient way of modulating future on-chip quantum interference experiments [6,8].

The structure is a Bragg reflection waveguide (BRW) capable of guiding modes from different frequency ranges by two distinct mechanisms [total internal reflection versus Bragg reflection from the claddings; see Fig. 1(a)] [18]. We use an analytical description of multilayer slab waveguides with periodic claddings to demonstrate that Bragg-guided modes of different polarization can be independently controlled by engineering the phase shift of the Fresnel reflection coefficient at the

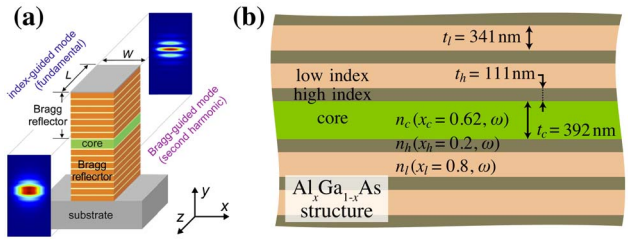

Fig. 1. (Color online) (a) Sketch of an $Al_xGa_{1-x}As$-based ridge BRW. (b) Enlarged view of the 1D slab BRW under study, showing its geometrical parameters.

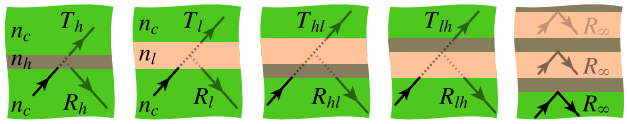

Fig. 2. (Color online) Illustration for the reflection and transmission coefficients used in Eqs. (2)–(5) (see text).

core/cladding interface. We derive the specific parameters for BRWs capable of switchable hyperentanglement and confirm our analytical results with fully vectorial two-dimensional (2D) numerical simulations [19]. The example designs are based on the $Al_xGa_{1-x}As$ platform, where self-pumped photon pair generation has been experimentally observed [20].

Consider a slab waveguide with a core surrounded on both sides by semi-infinite Bragg claddings made of alternating high- and low-index layers [Fig. 1(b)]. The existence condition for the guided modes in the core is

$$1 - R_\infty^2 \exp(2i\delta_c) = 0, \tag{1}$$

where R_∞ is the complex reflection coefficient of a semi-infinite Bragg cladding and $\delta_{i=c,l,h} \equiv w_i t_i$, with $w_i = (\omega/c)(n_i^2 - n_{\text{eff}}^2)^{1/2}$. To determine R_∞, we write the expressions for the complex reflection and transmission coefficient for a single high- and low-index layer surrounded by the core material, given by the Airy formulas

$$R_{i=h,l} = \frac{-r_{ic} + r_{ic}e^{2i\delta_i}}{1 - r_{ic}^2 e^{2i\delta_i}}, \qquad T_{i=h,l} = \frac{(1 - r_{ic}^2)e^{i\delta_i}}{1 - r_{ic}^2 e^{2i\delta_i}}, \tag{2}$$

where r_{ij} are the Fresnel reflection coefficients for the interface n_i/n_j. The reflection and transmission coefficients for one period of the cladding are (see Fig. 2)

$$R_{hl} = R_h + \frac{T_h^2 R_l}{1 - R_h R_l}, \qquad R_{lh} = R_l + \frac{T_l^2 R_h}{1 - R_h R_l}, \tag{3}$$

$$T_{hl} = T_{lh} = \frac{T_h T_l}{1 - R_h R_l}. \tag{4}$$

In a semi-infinite cladding, these coefficients are related to R_∞ as

$$R_\infty = R_{hl} + \frac{T_{hl} R_\infty T_{lh}}{1 - R_\infty R_{lh}}. \tag{5}$$

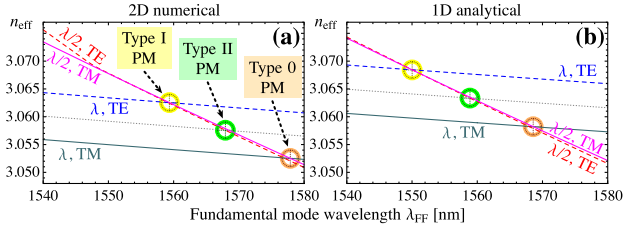

Fig. 3. (Color online) Dispersion curves for fundamental and second-harmonic modes showing type I, type II, and type 0 PM: (a) 2D simulation results for a ridge waveguide with $W = 4.4\,\mu$m; (b) analytical results for an infinite-period, 1D slab waveguide.

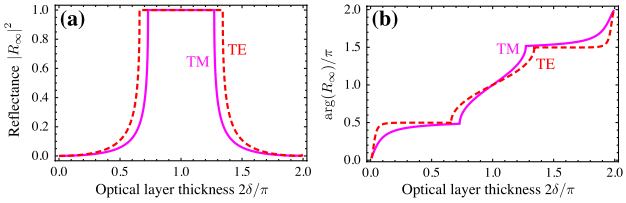

Fig. 4. (Color online) (a) Intensity and (b) phase of R_∞ for different $\delta = \delta_h = \delta_l$. The structure is as shown in Fig. 1.

For quarter-wave (QW) BRWs, $\delta_h = \delta_l = \pi/2$ and $R_\infty = -1$ [21], so Eq. (1) can be solved easily. Its solution should predict the dispersion properties of 2D ridge waveguides if $W \gg t_c$. This is indeed seen in Fig. 3. As expected, the mode effective indices are lower for a 2D ridge than for a one-dimensional (1D) slab (see [21]). In our case, this shift is ~0.005 for the index-guided modes and much less for the Bragg modes, so the wavelengths of all PM types are shifted by about 9 nm.

To bring several different PM types to the same wavelength, we need a means to shift the wavelength of different PM types independently with respect to one another. We show here that this can be achieved by veering the waveguide geometrical parameters off the QW condition.

Indeed, since the expressions for the interface Fresnel coefficients r_{ij} in Eq. (2) depend on polarization, namely, $r_{ij}^{\text{TE}} = (w_i - w_j)/(w_i + w_j)$ and $r_{ij}^{\text{TM}} = (w_i n_j^2 - w_j n_i^2)/(w_i n_j^2 + w_j n_i^2)$, the cladding reflection coefficient R_∞ is also polarization dependent. Figure 4 shows the dependence of R_∞ on $\delta \equiv \delta_h = \delta_l$. As expected, the reflectance of the cladding $|R_\infty|^2$ is unity inside its bandgap, with the phase $\arg(R_\infty)$ varying monotonically around π. The gap has different widths for TE- versus TM-polarized modes, so there is a mismatch in $\arg(R_\infty)$ whenever the cladding is operated outside the QW condition. According to Eq. (1), this phase mismatch results in a difference between n_{eff} for the two polarizations.

It can therefore be expected that any perturbation of the QW condition (a change in δ_h, δ_l, or δ_c) will create a controllable shift between n_{eff} for the TE versus TM polarization. Indeed, Fig. 5 shows how one can control $n_{\text{TE}} - n_{\text{TM}}$ for Bragg-guided modes by varying layer thicknesses. No polarization sensitivity is seen in the fundamental index-guided modes, so non-QW BRWs offer a means to control the effective index of Bragg-guided modes of different polarizations independently. This can be used to line up the wavelength of type II SPDC, which produces photon pairs entangled in both energy time and polarization, with the wavelength of type I or

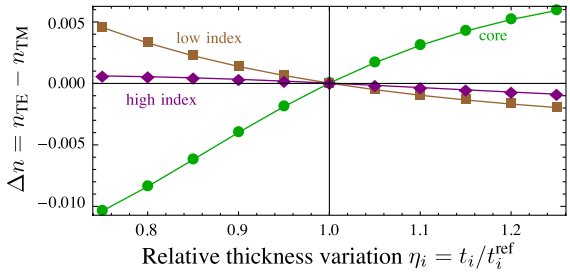

Fig. 5. (Color online) Dependence of $n_{\text{TE}} - n_{\text{TM}}$ for the zero-order Bragg mode of TE versus TM polarization on the variation of layer thicknesses $t_{c,l,h}$.

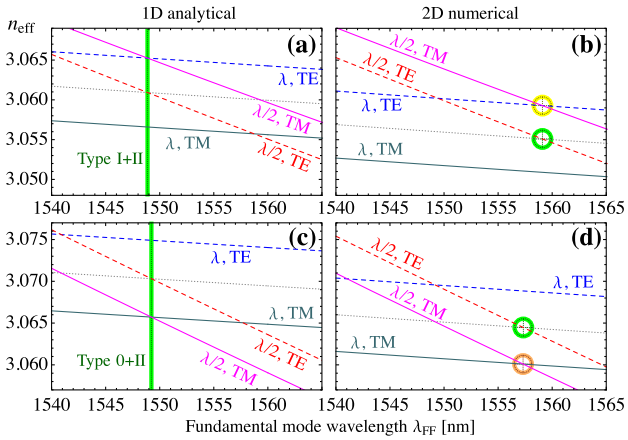

Fig. 6. (Color online) Dispersion relations of (a)–(b) structure with simultaneous type I and type II PM and (c)–(d) structure with simultaneous type II and type 0 PM. (a), (c) Analytical results for 1D slab waveguide with semi-infinite claddings, obtained from Eq. (5). (b), (d) Results from fully vectorial 2D simulation [19] for a ridge waveguide.

type 0 SPDC, either of which produces copolarized photon pairs having only time-energy entanglement.

To keep the PM wavelength near 1550 nm and to further enhance the difference between n_{TE} and n_{TM}, both t_c and t_l can be varied with opposite signs. The examples are shown in Fig. 6. The structure with t_c decreased by 33.2 nm and t_l increased by 50 nm (compared to the QW structure in Fig. 3) shows simultaneous PM for type I and type II SPDC [Fig. 6(a)]. The structure with t_c increased by 18.5 nm and t_l decreased by 64 nm shows simultaneous PM for type II and type 0 SPDC [Fig. 6(c)].

We have also verified our 1D results in 2D simulations [Figs. 6(b) and 6(d)]. For a moderate ridge width (4.4 μm), the property of multichannel PM is seen to persist in the 2D case with good accuracy, despite the systematic shifts in the effective index and PM wavelengths. For eight-period claddings, deviations from the QW condition cause an increase of radiation losses in the Bragg modes by several times. However, the losses do not exceed 0.2 dB/cm, which is acceptable in waveguides several millimeters long.

In summary, we have demonstrated that a single BRW structure can generate both time-energy entangled and hyperentangled photons by individual polarization control over the Bragg-guided modes in a non-QW BRW. By varying core and cladding layer thicknesses ($t_{c,l,h}$), the effective index difference between Bragg-guided modes of different polarizations ($n_{\text{TE}} - n_{\text{TM}}$) can be changed arbitrarily. We show analytically and confirm numerically that the proposed polarization control mechanism leads to simultaneous type I + type II or type II + type 0 SPDC. In both cases, simply rotating the polarization of the pump can switch between copolarized (time-energy entangled) and cross-polarized (hyperentangled with both polarization and time-energy entanglement) photon pair generation. Intermediate pump polarizations produce a coherent superposition of the two kinds of entanglement, providing a way to vary the degree of polarization entanglement in experiments dependent on it, e.g., Franson interferometry [6]. This may also be a precursor to observing multipartite continuous-variable entanglement in the infinite squeezing limit (see [22]).

The authors thank A. Branczyk, E. Zhu, and Y. Soudagar for fruitful discussions. This work was supported by the Natural Sciences and Engineering Research Council of Canada (NSERC).

References

1. T. D. Ladd, F. Jelezko, R. Laflamme, Y. Nakamura, C. Monroe, and J. L. O'Brien, Nature **464**, 45 (2010).
2. J. L. O'Brien, A. Furusawa, and J. Vučković, Nat. Photon. **3**, 687 (2009).
3. N. Gisin, G. Ribordy, W. Tittel, and H. Zbinden, Rev. Mod. Phys. **74**, 145 (2002).
4. K. Edamatsu, Jpn. J. Appl. Phys. **46**, 7175 (2007).
5. M. F. Saleh, G. Di Giuseppe, B. E. A. Saleh, and M. C. Teich, IEEE Photon. J. **2**, 736 (2010).
6. P. G. Kwiat, J. Mod. Opt. **44**, 2173 (1997).
7. D. V. Strekalov, T. B. Pittman, A. V. Sergienko, Y. H. Shih, and P. G. Kwiat, Phys. Rev. A **54**, R1 (1996).
8. J. T. Barreiro, N. K. Langford, N. A. Peters, and P. G. Kwiat, Phys. Rev. Lett. **95**, 260501 (2005).
9. C. Cinelli, M. Barbieri, R. Perris, P. Mataloni, and F. De Martini, Phys. Rev. Lett. **95**, 240405 (2005).
10. A. Hayat, P. Ginzburg, D. Neiman, S. Rosenblum, and M. Orenstein, Opt. Lett. **33**, 1168 (2008).
11. A. De Rossi, V. Ortiz, M. Calligaro, B. Vinter, J. Nagle, S. Ducci, and V. Berger, Semicond. Sci. Technol. **19**, L99 (2004).
12. S. M. Spillane, M. Fiorentino, and R. G. Beausoleil, Opt. Express **15**, 8770 (2007).
13. P. Abolghasem, M. Hendrych, X. Shi, J. P. Torres, and A. S. Helmy, Opt. Lett. **34**, 2000 (2009).
14. L. Sansoni, F. Sciarrino, G. Vallone, P. Mataloni, A. Crespi, R. Ramponi, and R. Osellame, Phys. Rev. Lett. **105**, 200503 (2010).
15. M. F. Saleh, G. Di Giuseppe, B. E. A. Saleh, and M. C. Teich, Opt. Express **18**, 20475 (2010).
16. C.-M. Li, K. Chen, A. Reingruber, Y.-N. Chen, and J.-W. Pan, Phys. Rev. Lett. **105**, 210504 (2010).
17. P. Abolghasem, J. Han, B. J. Bijlani, A. Arjmand, and A. S. Helmy, IEEE Photon. Technol. Lett. **21**, 1462 (2009).
18. A. S. Helmy, Opt. Express **14**, 1243 (2006).
19. Mode Solutions, version 4.0, Lumerical Solutions, Inc., http://www.lumerical.com/.
20. B. Bijlani, P. Abolghasem, A. Reijnders, and A. S. Helmy, in *CLEO:2011—Laser Applications to Photonic Applications*, OSA Technical Digest (CD) (Optical Society of America, 2011), paper PDPA3.
21. B. R. West and A. S. Helmy, J. Opt. Soc. Am. B **23**, 1207 (2006).
22. O. Pfister, S. Feng, G. Jennings, R. Pooser, and D. Xie, Phys. Rev. A **70**, 020302(R) (2004).